Supporting Information

Engineering Covalent Organic Frameworks for Enhanced Interfacial Lithium-Ion Flux Redistribution in Dendrite-Free Lithium-Sulfur Batteries

Tianli Li, Hua Hao, Jian Wang, Zhongzhi Yuan, Zhiyong Yu, and Hanxing Liu**

T. Li, H. Hao, Z. Yu, H. Liu

State Key Laboratory of Advanced Technology for Materials Synthesis and Processing, School of Material Science and Engineering, International School of Material Science and Engineering, Wuhan University of Technology, Wuhan 430070, China

J. Wang

Helmholtz Institute Ulm (HIU), Ulm D89081, Germany

Z. Yuan

South China Normal Univ, Sch Chem, Guangzhou 510006, Peoples R China

** Corresponding author*

E-mail: yuzhiyong@whut.edu.cn (Z. Yu); lhxhp@whut.edu.cn (H. Liu)

Physical Characterization:

The Raman spectra of the substances were studied using a Raman spectrometer (Raman, InVia). The elemental composition within the materials was documented utilizing X-ray photoelectron spectroscopy (XPS, ESCALAB-250Xi). The morphologies of as-prepared substances were characterized by scanning electron microscopy (SEM, JSM-IT300) and transmission electron microscopy (TEM, Talos-F200S). The contact angle of various separators was studied utilizing a contact angle instrument (JC2000C optical). The UV-Vis absorption spectra were assessed using a Perkin Elmer Lambda spectrophotometer, while the crystalline structure of the materials was examined via X-ray diffraction analysis (XRD, Bruker D8).

Electrochemical measurement:

The electrochemical properties were assessed using CR2025 coin cells assembled with a CNT/S cathode, a metallic lithium anode, and a separator modified with either fBTTP-COF, tBTTP-COF, or PP. The electrolyte was prepared by dissolving 1.0 M lithium bis(trifluoromethanesulfonimide) (LiTFSI) salt and 2 wt% $LiNO_3$ in a 1:1 volume ratio mixture of 1,3-dioxolane (DOL) and dimethoxyethane (DME). Galvanostatic charge-discharge tests were conducted on a Land battery testing system (Wuhan LAND Electronic Co., Ltd.) within a voltage range of 1.7 to 2.8 V. Cyclic voltammetry (CV) curves were obtained using a CHI760E electrochemical workstation (Chenhua Instrument, Shanghai) at scan rates ranging from 0.1 to 0.5 mV s^{-1}. Electrochemical impedance spectroscopy (EIS) measurements were recorded over a frequency range of 100 kHz to 0.01 Hz with an amplitude of 5 mV. All battery assemblies were carried out in an argon-filled glovebox.

Li^+ diffusion coefficient:

The diffusion coefficient of Li^+ ions was determined using the Randles-Sevcik equation:

$$I_p = (2.69 \times 10^5) n^{1.5} A D_{Li}^{+0.5} v^{0.5} C_{Li}$$

where Ip signifies the peak current, n represents the number of electron transfers (n = 2), A denotes the electrode's surface area, D_{Li}^+ stands for the Li^+ diffusion coefficient, C_{Li} indicates the concentration of Li^+ ions, and v refers to the CV scan rates ranging from 0.1 to 0.5 mV s^{-1}. A linear correlation was observed between I_p and the square root of the scan rate ($v^{1/2}$).

Assembly of Li_2S_6 symmetric cells:

For the Li_2S_6 symmetric battery testing, both the working electrode and the counter electrode were identical, comprising 75% active material (either fBTTP-COF, or tBTTP-COF alone), 15% carbon black for conductivity enhancement, and 10% PVDF as a binder. The prepared Li_2S_6 solution served as the electrolyte, battery assembly was performed in an Ar-filled glovebox. CV measurements were performed within a potential window of -0.1 V to 0.1 V at a scan rate of 2 mV s^{-1}.

Visualized adsorption of polysulfides:

A homogeneous solution was obtained by thoroughly dissolving a mixture of Li_2S and S powders in a 1:5 molar ratio in a 1:1 volume ratio of DME and DOL, with agitation for 24 h. Subsequently, identical quantities of fBTTP-COF and tBTTP-COF were introduced into equal amounts of Li_2S_6 solution. To ascertain and validate the adsorption capacity of the synthesized materials for Li_2S_6, Ultraviolet-visible (UV-vis) spectroscopy was employed to analyse the adsorptivity of as-prepared samples.

Measurement for the Li_2S deposition:

Li_2S_8 solution was formulated by dissolving Li_2S and S in a 7:1 molar ratio within a DOL/DME solvent blend (1:1 ratio), followed by stirring at 60°C for 24 h. The

cathode was fabricated using carbon cloth (CC) as the current collector, onto which fBTTP-COF or tBTTP-COF was deposited. For the cathode, a specific electrolyte was prepared containing 0.25 M Li_2S_8 and 1.0 M LiTFSI in Tetraglyme ether. Conversely, the anode employed a distinct electrolyte consisting solely of 1.0 M LiTFSI, excluding Li_2S_8. The assembled battery underwent an initial discharge at 0.112 mA until it reached 2.06 V, followed by a maintenance phase at a constant voltage of 2.05 V to facilitate the growth of Li_2S.

DFT calculation:

First-principles calculations based on Density Functional Theory (DFT) were carried out using the Projected Augmented Wave (PAW) approach, which was an integral part of the Vienna Ab initio Simulation Package (VASP). These calculations employed the generalized gradient approximation (GGA) in conjunction with the Perdew-Burke-Ernzerhof (PBE) functional, alongside the PAW potential. A kinetic energy cut-off of 450 eV was specified. Convergence criteria were established at 0.02 eV $Å^{-1}$ and 10^{-4} eV for energies. To ensure the isolation of periodic images, a generous vacuum region of 15 Å was introduced across all systems. The charge density difference was derived by computing the charge disparity between the substrate and the adsorbent.

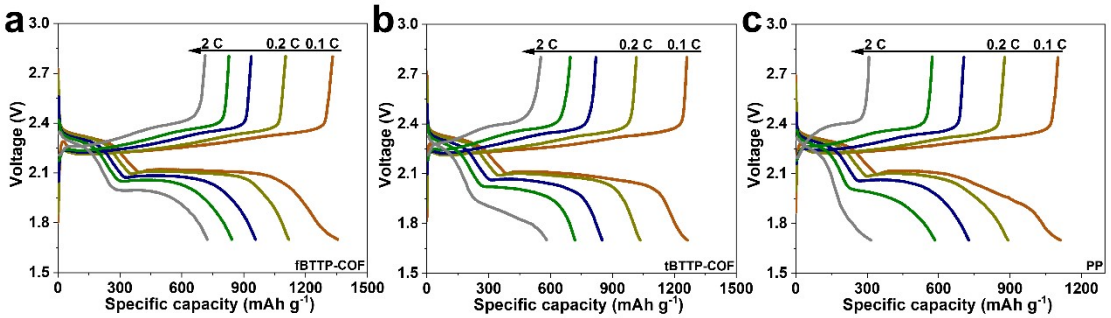

Figure S1. Charge-discharge profiles of the fBTTP-COF a), tBTTP-COF b), and PP c) separators-based batteries at different rates.

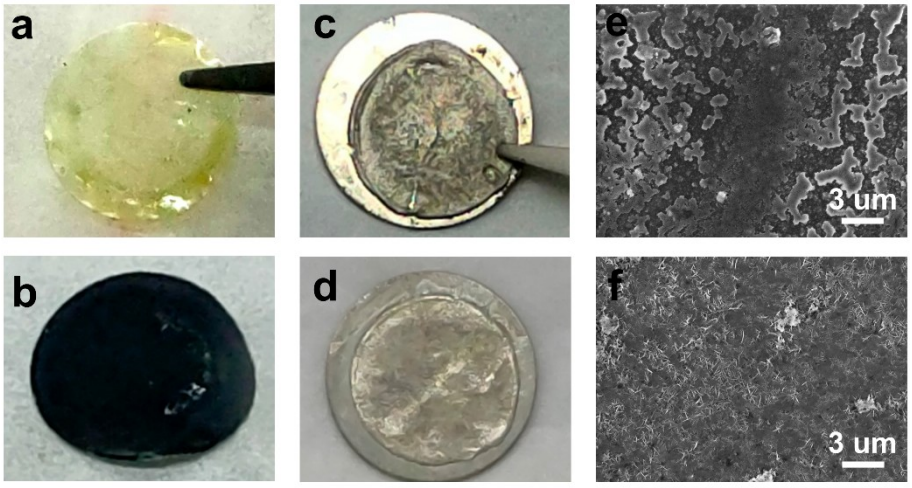

Figure S2. Photographs of the separators and lithium anode of a, c) PP and b, d) fBTTP-COF. SEM images of the lithium anode with e) PP and f) fBTTP-COF after cycling.

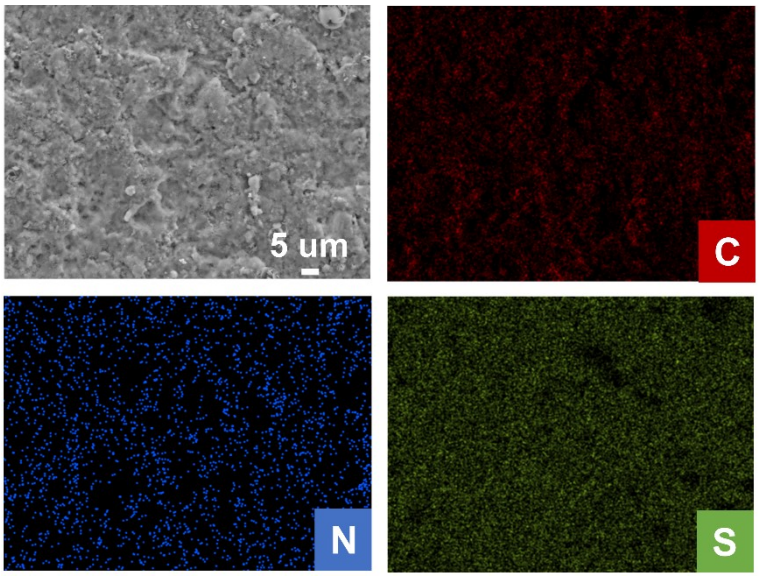

Figure S3. Elemental mapping images of fBTTP-COF separator after cycling.

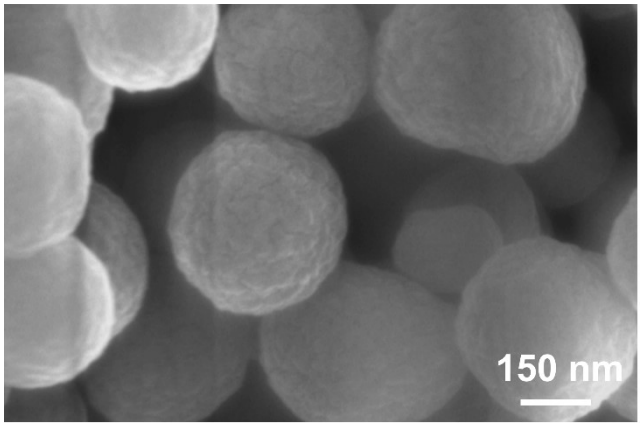

Figure S4. SEM images of fBTTP-COF after cycling.

Table S1. Summary of slope at peak C, A', and A" for different separators

Modified separator	**PP**	**tBTTP-COF**	**fBTTP-COF**
Sloop at peak C ($cm^2\ s^{-1}$)	0.15000	0.28730	0.29356
Sloop at peak A' ($cm^2\ s^{-1}$)	0.06360	0.10028	0.13508
Sloop at peak A" ($cm^2\ s^{-1}$)	0.06350	0.10156	0.15042

Table S2. Summary of lithium-ion diffusion coefficient (D_{Li+}) for various separators

Modified separators	**PP**	**tBTTP-COF**	**fBTTP-COF**
D_{Li+} at peak C ($cm^2\ s^{-1}$)	4.798×10^{-8}	1.716×10^{-7}	1.838×10^{-7}
D_{Li+} at peak A' ($cm^2\ s^{-1}$)	8.627×10^{-9}	2.145×10^{-8}	3.891×10^{-8}
D_{Li+} at peak A" ($cm^2\ s^{-1}$)	8.600×10^{-9}	2.200×10^{-8}	4.825×10^{-8}

Table S3. electrochemical performance comparison between reported works and fBTTP-COF modified separator-based Li-S batteries.

Modified Separators	**Coating loading (mg cm^{-2})**	**Sulfur loading (mg cm^{-2})**	**Rate capacity (mAh g^{-1})/C rate**	**Capacity decay rate/ cycle number**	**Ref.**
VN	1.52	1.6	895/1 C	0.077%/800	[1]
Nb_2O_5-CNT	0.38	1.4	552/0.2 C	0.23%/100	[2]
N, S–Mo_2C/C-ACF	0.5	0.9-1.3	900/1 C	0.08%/600	[3]
TiO/MWCNTs	0.7	1.4-1.6	1247.2/0.5 C	0.057%/1000	[4]
A/R-TiO_2	0.23	1.4	920/1 C	0.055% /800	[5]
Ni-Co-P@C	0.4	1.8	961.3/0.5 C	0.056%/1000	[6]
C_3N_4-$CoSe_2$	0.5	1.5	923.7/1 C	0.0819%/500	[7]
SCOF-2	0.15	1.3-1.5	795/1 C	0.4%/800	[8]
fBTTP-COF	**0.35**	**1.41**	**888.3/1 C**	**0.037%/700**	**This work**

References

1 Y. Song, S. Zhao, Y. Chen, J. Cai, J. Li, Q. Yang, J. Sun and Z. Liu, *ACS Appl. Mater. Interfaces*, 2019, **11**, 5687-5694.

2 Y. Liu, M. Chen, Z. Su, Y. Gao, Y. Zhang and D. Long, *Carbon*, 2021, **172**, 260-271.

3 H. Li, Q. Jin, D. Li, X. Huan, Y. Liu, G. Feng, J. Zhao, W. Yang, Z. Wu, B. Zhong, X. Guo and B. Wang, *ACS Appl. Mater. Interfaces*, 2020, **12**, 22971-22980.

4 Z. Li, L. Tang, X. Liu, T. Song, Q. Xu, H. Liu and Y. Wang, *Electrochim. Acta.*, 2019, **310**, 1-12.

5 L. Ma, Y. Zhang, S. Zhang, L. Wang, C. Zhang, Y. Chen, Q. Wu, L. Chen, L. Zhou and W. Wei, *Adv. Funct. Mater.*, 2023, **33**, 2305788.

6 Z. Wu, S. Chen, L. Wang, Q. Deng, Z. Zeng, J. Wang and S. Deng, *Energy Storage Mater.*, 2021, **38**, 381-388.

7 Z. Liang, C. Peng, J. Shen, J. Yuan, Y. Yang, D. Xue, M. Zhu and J. Liu, *Small*, 2024, **20**, 2309717.

8 J. Xu, S. An, X. Song, Y. Cao, N. Wang, X. Qiu, Y. Zhang, J. Chen, X. Duan, J. Huang, W. Li and Y. Wang, *Adv. Mater.*, 2021, **33**, 2105178.